Design of a Remote Control System for a Wireless Microrobot

Philippe Basset
IEMN-Dpt ISEN
UMR CNRS 8520
philippe.basset@isen.fr

Andreas Kaiser
IEMN-Dpt ISEN
UMR CNRS 8520
andreas.kaiser@isen.fr

Bruno Steffaneli
IEMN-Dpt ISEN
UMR CNRS 8520
bruno.steffaneli@isen.fr

Dominique Collard
CIRMM/IIS-The University of Tokyo
dominique.collard@iemn.univ-lille1.fr

Lionel Buchaillot
IEMN-Dpt ISEN
UMR CNRS 8520
lionel.buchaillot@isen.fr

Abstract

The design of the components for the remote control of a microrobot is presented. The robot consists in a high Q antenna, a high voltage circuit and a distributed system of electrostatic actuators, realizing a Ciliary Motion System (CMS) [1]. The received voltage on the antenna, obtained by inductive coupling at 1cm, is 100V on a 1kΩ load. This allows both microsystem actuation (80V with a 380 µm piece of silicon as a load) and the powering of the circuit. The high voltage circuit has been designed in the Alcatel-Mietec I2T100 technology. It is able to drive two CMS in order to obtain a remote motion system with two degrees of freedom. The circuit has been succesfully simulated with a 250 pF load.

1. Introduction

The realization of an autonomous microrobot is a significant challenge for the future. Many applications are expected particularly in the field of the microassembly and the test of circuits in confined environement. [2]. The project presented in this paper consists of a Ciliary Motion System (CMS) [1] with a remote actuation obtained by inductive coupling. An overview of the system is shown in figure 1.

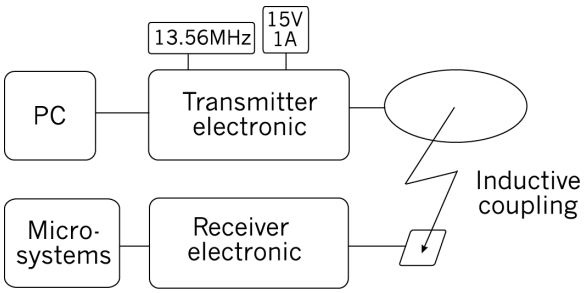

Figure 1: Overview of the system.
The emitter card provides a 1A/15V current, modulated in amplitude by the PC, through the emitter antenna. The power transmitted by inductive coupling feeds a high voltage control circuit, allowing the electrostatic actuation of the microsystems.

The actuators of the CMS are build from self assembling polysilicon process [3] with an additional level of polysilicon. The actuation voltage is 80V. The principle is shown in figure 2. A detailed description can be found in [4]. The receiver antenna has been fabricated on an epoxy substrate [5]. This results in the weight the robot has to support being minimized and the prevention of the losses due to Eddy currents, as well as the substrate parasitic capacitance is reduced. Its design has been optimized in order to maximize the energy transfer.

To obtain two degrees of freedom, two CMS must be controlled independantly. So four signals are needed simultaneously. To apply the right command to the right set of actuators, a high voltage circuit capable of driving high capacitive loads has been designed using the Alcatel-Mietec I2T100 technology.

2. Design of the antenna

2.1. Fabrication

The process of the antenna fabrication is shown in

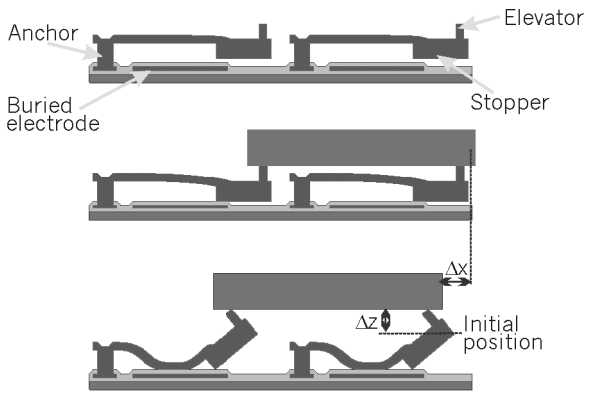

Figure 2: The actuator principle.
The voltage applied on the burried electrode enables the pull-in of the moving part toward the substrate due to electrostatic forces. When the stopper contacts the substrtate, an axis of torsion is created which forces the plate's free end to raise.

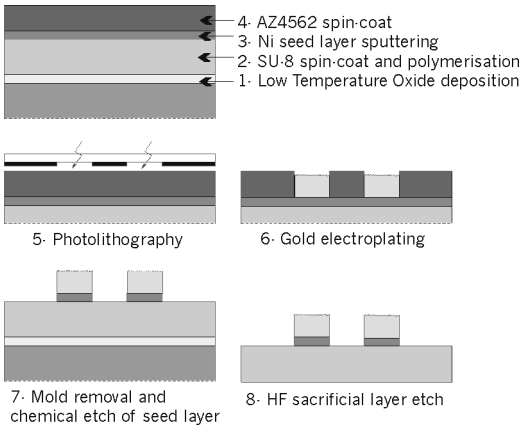

Figure 3: Process flow of the receiver antenna.

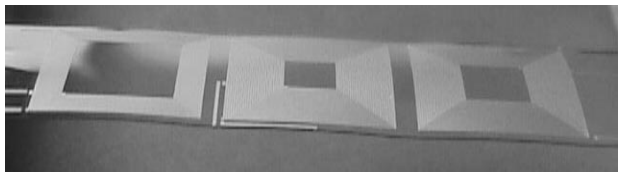

	Antenna 1	Antenna 2	Antenna 3
L (mH)	5.8	7.8	7.2
Self Resonance Frequency (MHz)	54	49	62
C (pF)	1.5	1.3	0.92
Q_L (13.56 MHz)	19	27	29
Q_L max	27 (27MHz)	32 (15.5MHz)	37 (19MHz)

Figure 4: a- Pictures of antennas
b- Sum-up of their characteristics

figure 3. On a sacrificial oxide layer, 150 µm of an epoxy resist are deposited. Once polymerized, the film will become a flexible, tough and light substrate. 24 µm of gold are electroplated in a positive resist mold. Finally the epoxy film is separated from the wafer using hydrofluoric acid.

2.2. Measurement and Q-factor extraction

One-port S parameters were measured from 30 KHz to 100 MHz and converted to impedance Z_L. Then the parasitic capacitance *Cp* of the test device was de-embedded using open calibration of the device. Parameter extraction is deduced from an equivalent circuit consisting of a capacitor *C* with a series of an inductance *L* and a resistor *R*. To extract *L* and *C* some assumptions need to be made.

As frequency increases, the penetration of the magnetic field into the conductor is attenuated (skin effect), which causes a reduction in the magnetic flux internal to the conductor. However, *L* does not decrease significantly with increasing frequency because it is predominantly determined by the magnetic flux external of the conductor [6]. Thus, *L* can be approximated as constant with frequency. *C* is considered to be independent of frequency since it represents the metal-to-metal overlap capacitance between the turns. *L* is extracted from low-frequency imaginary part of Z_L and *C* using the low-frequency *L* value and the resonance frequency of the antenna. The quality factor Q_L is estimated by taking the ratio of the imaginary and real parts of the one-port impedance, observing Z_L as purely inductive in the frequency range of interest. Results are summed up in figure 4b.

3. Energy transfer optimization

3.1. Receiver micro coil optimization

For the circuit in figure 5, assuming a sinusoidal alternating current i_1 and the receiver antenna tuned with the emitter frequency ω_0, the relationship between the induced voltage u_2 and the magnetic coupling of antennas (in the non complex form) is given by [7]:

$$u_2 = \frac{\omega_0 \cdot k\sqrt{L_1 L_2}}{\sqrt{\left(\frac{r_2}{R_L}\right)^2 + \omega_0^2 \cdot \left(C_2 \cdot r_2 + \frac{L_2}{R_L}\right)^2}} \cdot i_1 \qquad (1)$$

where *k* is the coupling factor between antennas, r_2 the serial losses of L_2, and $\omega_0 = 1/(L_2.C_2)^{1/2}$.

By substituting L_1, L_2, k and r_2 with the appropriate expressions [4], induced voltage simulations show an optimum turn number for a given hollow-coil area and load value (figure 7). This optimum, corresponding to the highest value of the inductance while keeping its serial losses at minimum, depends of the consumed current. Indeed, the more the load decreases, the more the influence of the electrical resistance of L_2 is prevalent. For an infinite load, the optimum turn number corresponds to a whorl width equivalent to the space between them.

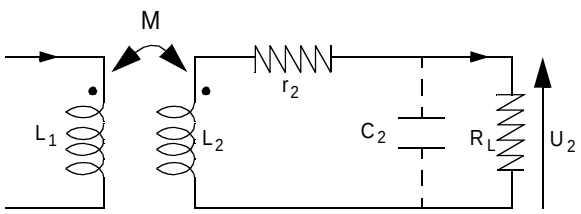

Figure 5: Electrical model of antennas

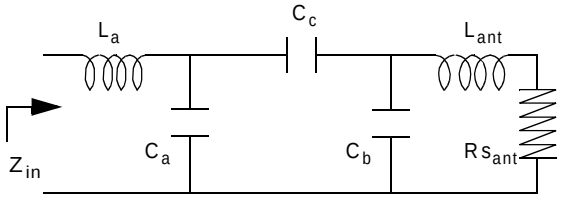

Figure 6: Schematic of the impedance matching circuit

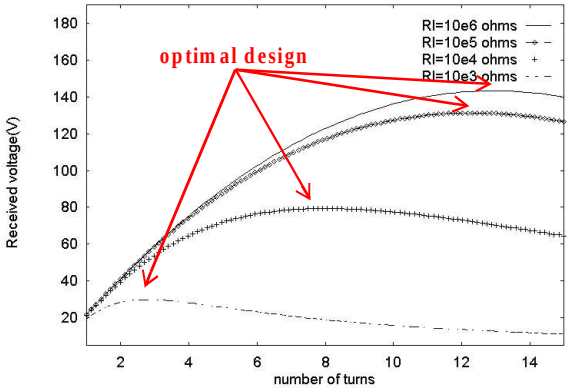

Figure 7: Simulation of induced voltage for a given hollow coil versus the loop number of identically spaced whorls.

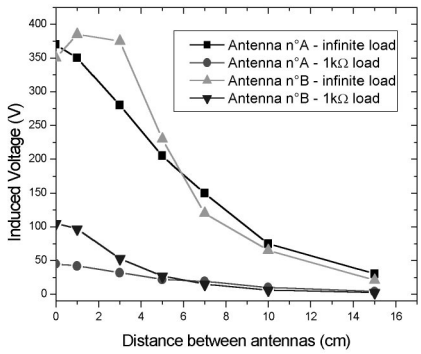

Figure 8: Measured peek to peek induced voltage on antenna #3 tuned at 13.56 MHz with two transmitter antenna. Antenna A: 2 turns, 14 cm diameter. Atenna B: 4 turns, 7 cm diameter.

3.2. Impedance matching of transmitter antenna

The dimensions of the transmitter antenna have also a serious effect on the induced power. Reducing its diameter increases the received voltage but only for small distances, since the coupling factor k is then closer to 1. Another important point to consider is the impedance matching between the antenna and the electrical circuit which has to provide the modulated AC current i_1. The L-C network proposed in figure 6, called T-match [8], allows all kinds of impedance matching. Having symmetrical components as L_a=L_{ant} and C_a=C_b guarantees Z_{in} being purely resistive. The presence of C_c permits to gain one degree of freedom and to state independent equations for C_a and C_c, depending on Rs_{ant}, $Z_{in,}$ and ω_o.

3.3. Experimental results

At the emission, an electronic card is able to provide an AC current up to 1A/18V through the transmitter antenna. The card is controlled by a computer that modulates the current amplitude in real time. The receiver antenna is tuned to the operating frequency 13.56 MHz with a discrete capacitor. The induced voltage as a function of distance for two transmitter antennas is reported in figure 8.

4. Design of the high voltage circuit

The circuit was conceived for the Alcatel-Mietec I2T100 technology which supports voltages up to 100V thanks to the use of DMOS transistors. The block diagram of figure 9 shows the principal functionalities of the circuit.

4.1. Analog Part

The signal received by the antenna must be between 20 and 25V peak. The actuation voltage of the microsystems is obtained from a Cockcroft-Walton rectifier/quadruplor. As a precaution, a device limiting the voltage to 100V is implemented. A 5V regulator and a clock generator allow the operation of the digital block. The signal is recovered using a simple envelope detector,

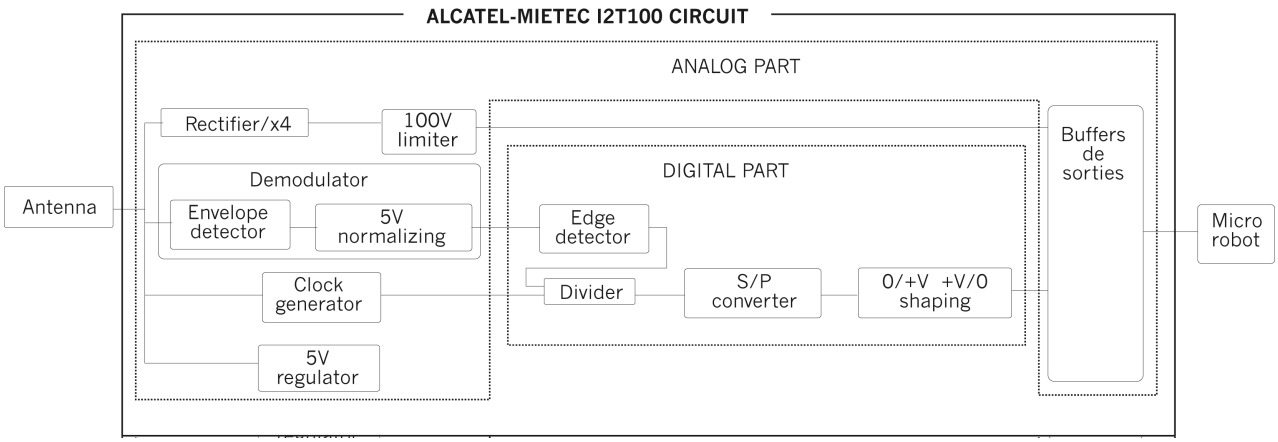

Figure 9: Block schematic of the high voltage circuit

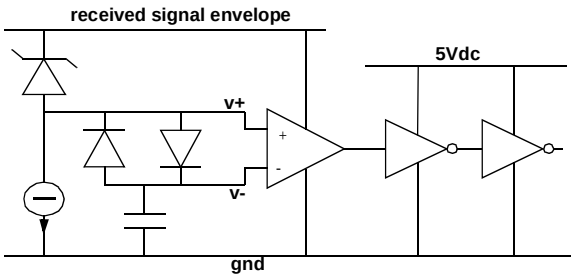

Figure 10: Simplified schematic of the demodulator. The signal envelope is applied to the positive output of a differential pair and compared to a voltage ranging between the peak and bottom level.

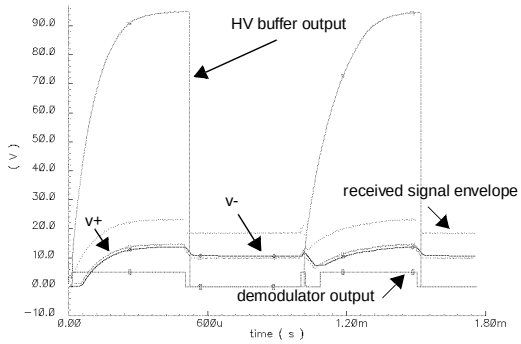

Figure 11: Spectre simulation of the analog part

then converted to 5V by a differential pair comparing the envelope with an average voltage ranging between the peak and bottom levels of the signal (figure 10). The description of the output buffer can be obtained in [9].

4.2. Digital part

A frequency divider reconverts the clock of 13.56MHz to 10kHz. A reset of the divider occurrs at each front detection in order to constantly synchronize the data with the clock. The serial/parallel conversion of the data is carried out according to the principle of a very simplified UART. The actuation of the robot requires 4 simultaneous bits of information. Those are encapsulated in 4 bits of protocol and continually sent into a shift register. At each clock period the protocol bits are checked. If they are recognized as being valid, the data are read (figure 12).

During the charging of the capacitive load, the received voltage drops due to the high power consumption. To avoid errors on the high voltage output, the data transmission from the analog to the digital circuit is disabled for that time.

In order to avoid the stiction of the actuators to the substrate because of charge accumulation in the device, a last block applies the output voltage alternatively to the moving part and the burried electrode.

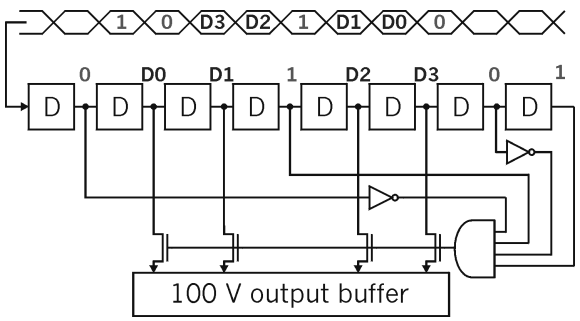

Figure 12: Simplified schematic of the serial/parallel converter. The data are encapsulated to be transmitted to the output buffer only when the shift register is correctly filled.

4.3. Results of simulation

Simulations showed the operation of the circuit for a sinusoidal entry of 20V peak at 13.56MHz, modulated with 1kHz and a capacitive load of 250pF.

5. Conclusion

Concerning the four steps in wireless microrobot conception which are the remote powering, the actuator realization, the control circuit design and the packaging of the components, two have already been experimentally checked. The high voltage circuit has been validated by simulation and will be tested soon.Work on the packaging is in progress, in particular about the way to connect the circuit to the actuators.

6. references

[1] M. Ataka, A. Omodaka, N Takeshima and H. Fujita, "Fabrication and operation of polyimide bimorph actuators for a ciliary motion system", *JMEMS*, vol. 2, n°4, dec. 1993, pp. 146-50.

[2] M. Takeda, "Application of MEMS to industrial inspection", *Proceeding of MEMS'01*, pp. 182-91.

[3] T. Akiyama, D. Collard, and H. Fujita, "Scratch Drive Actuator With Mechanical Links for Self-Assembly of Three-Dimensional MEMS", *JMEMS*, vol. 6, no. 1, Mar. 1997, pp 10-17.

[4] P. Basset, A. Kaiser, P. Bigotte, D. Collard and L. Buchaillot, "A large stepwise motion electrostatic actuator for a wireless microrobot", *Proceeding of MEMS'02*, pp. 606-609

[5] P. Basset, A. Kaiser, D. Collard and L. Buchaillot, "Process and realization of a 3D gold electroplated antenna on a flexible epoxy film for a wireless micro motion system", *to be published in JVST B*, manuscript #20131

[6] C. P. Yue and S. S. Wong, "On-chip spiral inductors with patterned ground shields for Si-based RF IC's", *JSSC*, vol. 33, n°5, pp. 743-7, may 1998

[7] K. Finkenzeller, *RFID handbook*, John Wiley & son, 1999, p. 68.

[8] T. H. Lee, *The design of CMOS radio frequency integrated Circuit*, Cambridge University Press, 1998, p. 49.

[9] B. Stefanelli, Y. Mita, A. Kaiser, and H. Fujita, "A 32bit 100V switching array IC ready-to-use for everyone through multi-chip foundry srevice", *Proceeding Transducer'99*